Supporting Information

Morphology control of anatase TiO_2 for well-defined surface chemistry

Gabriel Jeantelot,[a] Samy Ould-Chikh,*[a] Julien Sofack-Kreutzer,[a] Edy Abou-Hamad,[a] Dalaver H. Anjum,[b] Sergei Lopatin,[b] Moussab Harb,[a] Luigi Cavallo[a] and Jean-Marie Basset*[a]

[a] Kaust Catalysis Center (KCC), Physical Science and Engineering Division (PSE), King Abdullah University of Science and Technology (KAUST), Thuwal 23955-6900, Saudi Arabia

[b] Imaging and Characterization Lab, King Abdullah University of Science and Technology, Thuwal 23955-6900, Saudi Arabia.

KEYWORDS: Titanium dioxide, Anatase, morphology, surface hydroxyls, fluorine, NMR, DFT, FT-IR, SOMC

The TEM surface area and 001 surface proportion are given by the following equations:

$$\tan(\alpha) = \frac{c}{a}$$

$$S_{\{101\}} = 2\sqrt{1+\tan^2(\alpha)} * \left(l_{[100]}^2 - \left(l_{[100]} - \frac{l_{[001]}}{\tan(\alpha)}\right)^2\right)$$

$$S_{\{001\}} = 2\left(l_{[100]} - \frac{l_{[001]}}{\tan(\alpha)}\right)^2$$

$$S_{tot} = S_{\{001\}} + S_{\{101\}}$$

$$V = \frac{\tan(\alpha)}{3} * \left(l_{[100]}^3 - \left(l_{[100]} - \frac{l_{[001]}}{\tan(\alpha)}\right)^3\right)$$

$$\rho = \frac{4 * M_{TiO_2}}{c * a^2 * N_a}$$

$$A_{TEM} = \frac{S_{tot}}{\rho * V}$$

$$\%\{001\} = \frac{S_{\{001\}}}{S_{tot}}$$

With $\mathbf{N_a}$ Avogadro's constant, $\mathbf{M_{TiO2}}$ the molar mass of TiO_2, **c** and **a** the unit cell parameters of anatase, **ρ** the density of anatase, **α** the angle between the (001) and (101) planes, $\mathbf{l_{[100]}}$ the average length of a particle along the [100] axis, $\mathbf{l_{[001]}}$ the average length of a particle along the [001] axis, $\mathbf{S_{\{101\}}}$ the average surface of a particle on {101} facets, $\mathbf{S_{\{001\}}}$ the average surface of a particle on {001} facets, **S_{tot}** the average total surface of a particle, **A_{TEM}** the TEM surface area, **%{001}** the proportion of {001} facets in the total particle surface.

{101}-anatase synthesis:

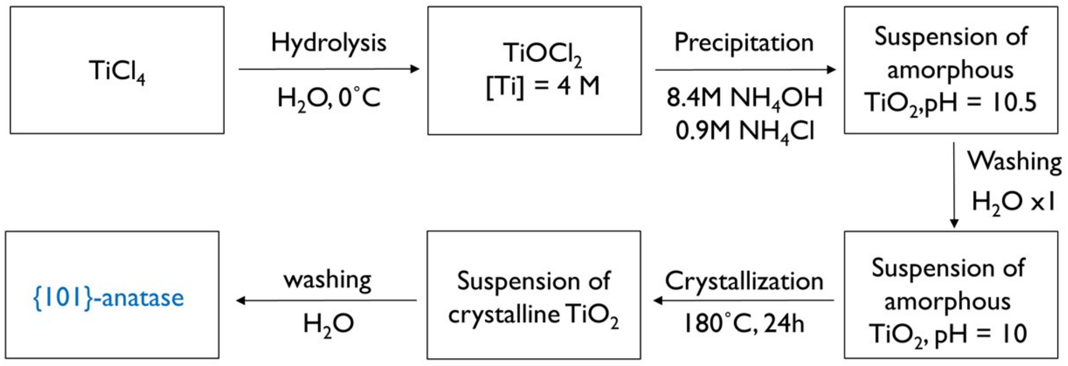

{001}-anatase synthesis:

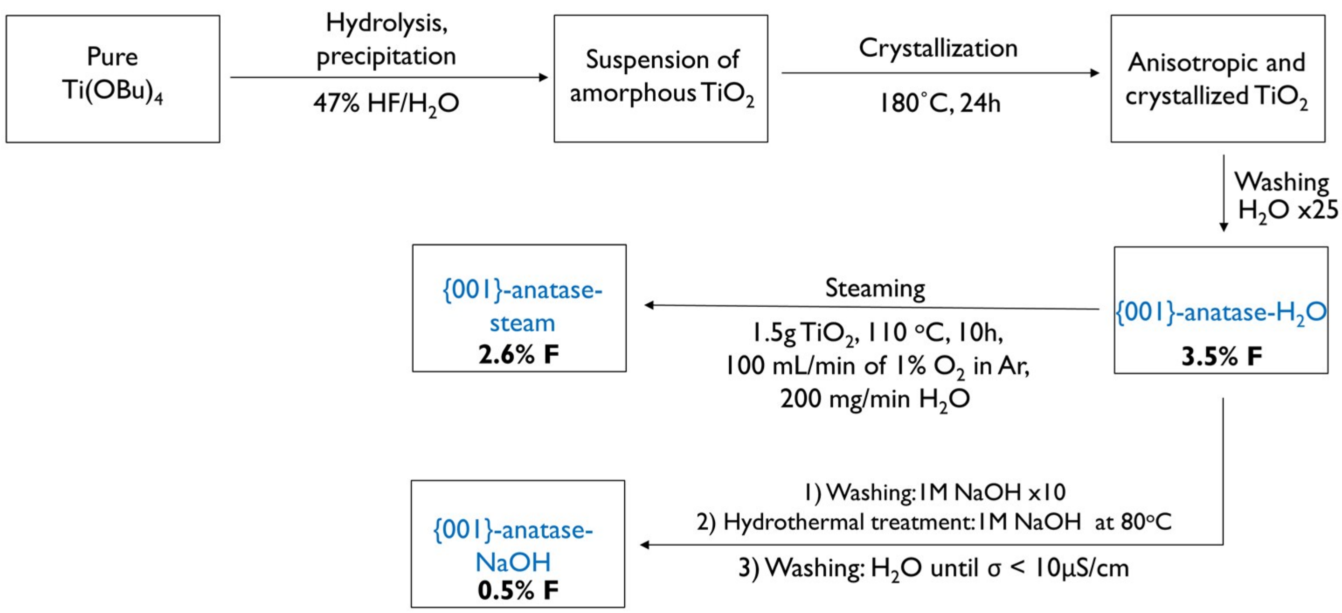

Fig. S1 Schematic representation of the syntheses of anatase samples used in this study

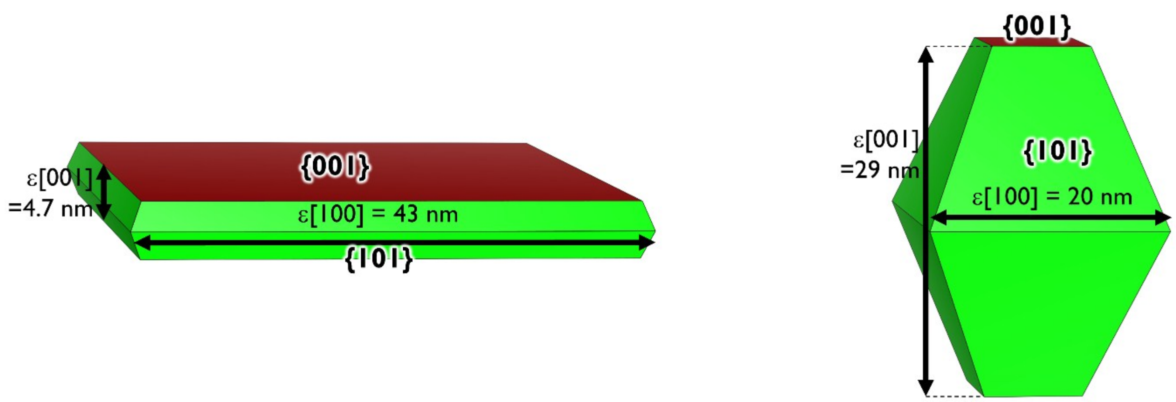

Fig. S2 Average shape of {001}-anatase (left) and {101}-anatase, based on TEM measurments.

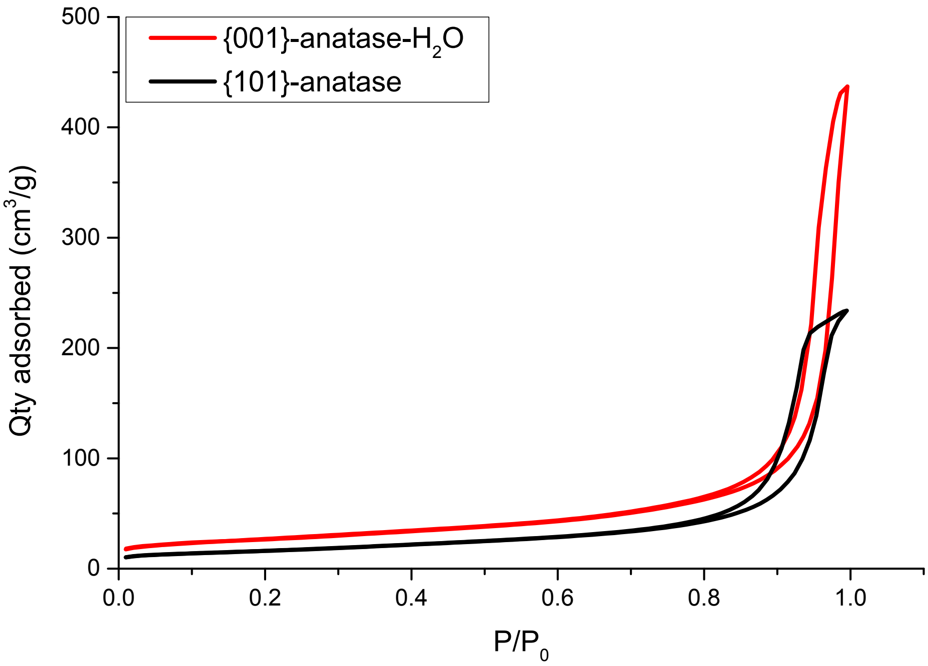

Fig. S3 BET N2 adsorption isotherms of {001}-anatase-H_2O and {101}-anatase

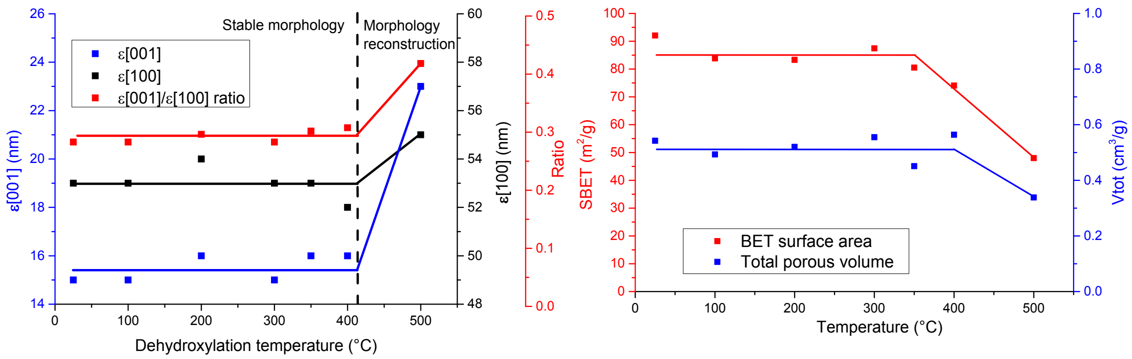

Fig. S4 Evolution of the [001] and [100] XRD coherent domains (left) and BET surface area and porous volume (right) of {001}-anatase against dehydroxylation temperature

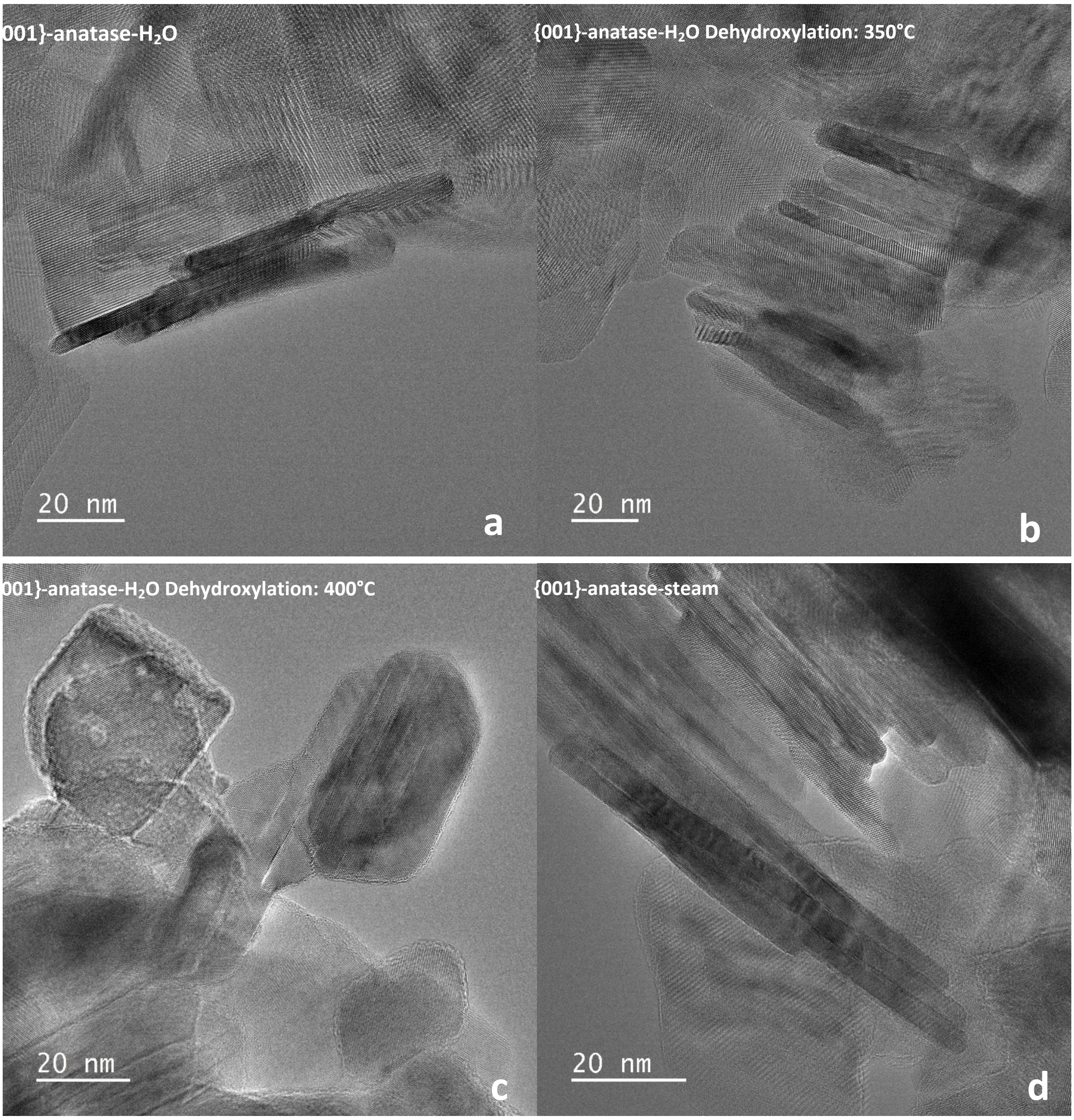

Fig. S5 TEM micrographs of {001}-anatase. **a)** {001}-anatase-H_2O **b)** {001}-anatase-H_2O after dehydroxylation at 350°C. No alteration is visible. **c)** {001}-anatase-H_2O after dehydroxylation at 400°C. Platelets become fused together and devellop crystallographic holes **d)** {001}-anatase-steam. No alteration is visible relative to {001}-anatase-H_2O

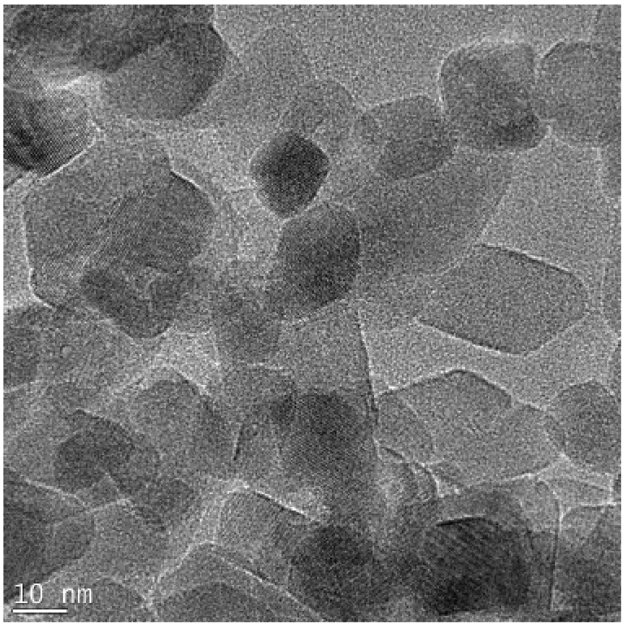

Fig. S6 TEM micrograph of {101}-anatase.

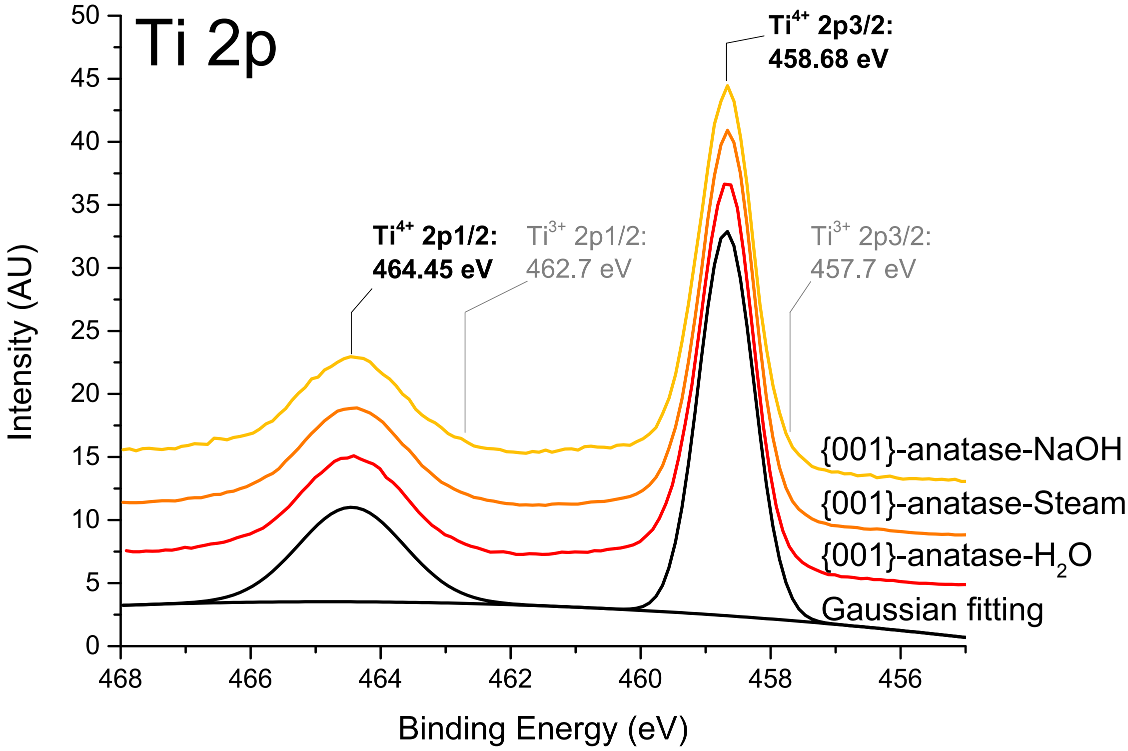

Fig. S7 XPS spectra showing the Ti ^{2}p binding energies of {001}-anatase samples and their gaussian fitting : only Ti^{4+} are seen, with Ti^{4+} 2p1/2 and 2p3/2 binding energies of 464.45 eV and 458.68 eV respectively. No Ti^{3+} 2p1/2 or 2p3/2 peaks are seen at 462.7 or 457.7 eV.[1–3]

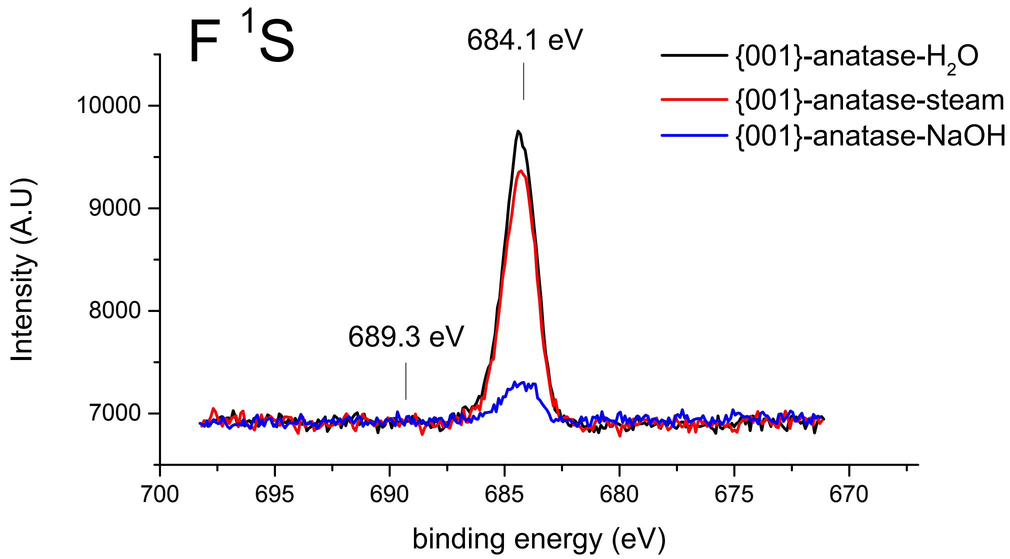

Fig. S8 XPS spectra showing the F [1]S binding energy of {001}-anatase samples

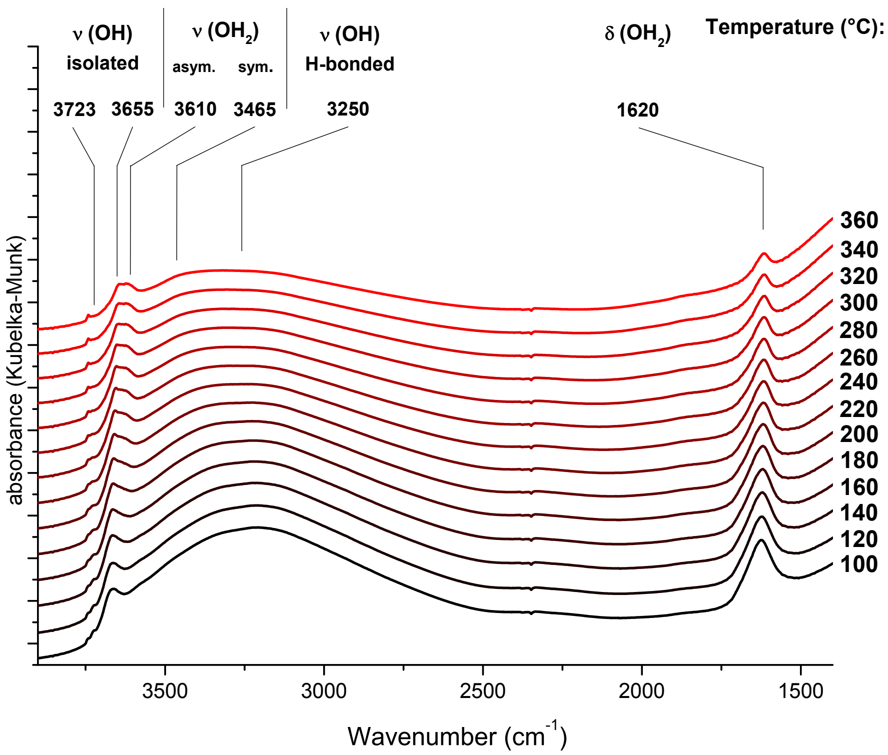

Fig. S9 In-situ DRIFTS of {001}-anatase-H_2O under flow of 20% oxygen in argon at varying temperature

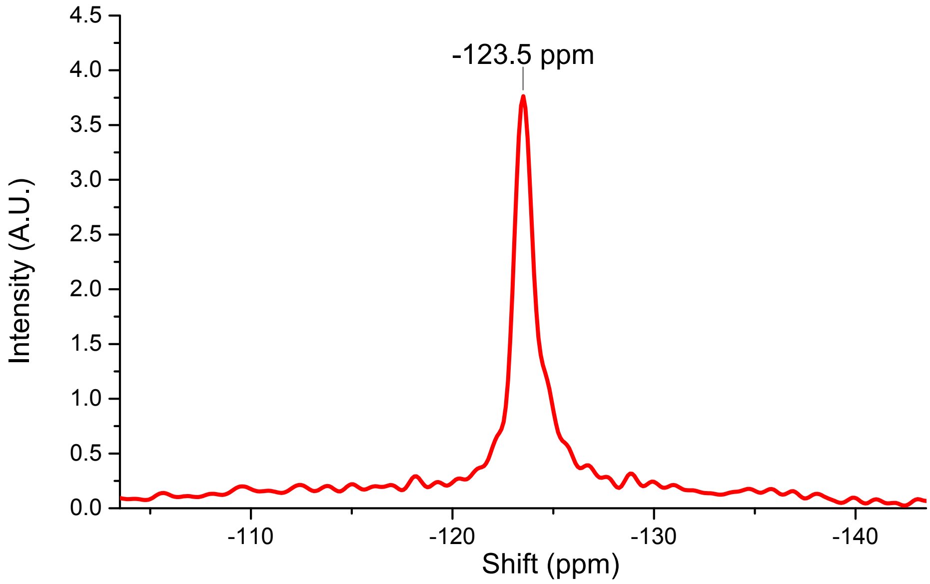

Fig. S10 ^{19}F MAS SSNMR of sample {001}-anatase-steam after dehydroxylation at 200°C

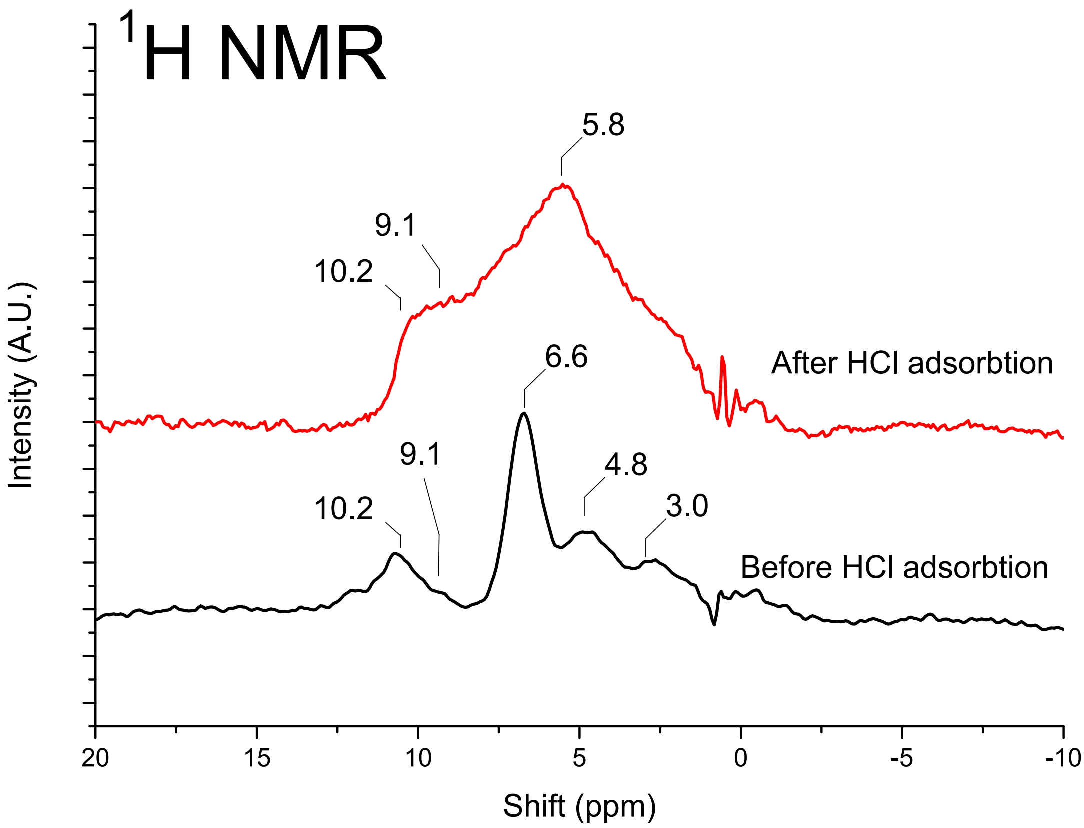

Fig. S11 1H MAS SSNMR of sample {001}-anatase-steam dehydroxylated at 200°C before and after adsorbtion of gaseous HCl (1 bar HCl for 5h, 10^{-5} mbar dynamic vacuum for 12h).

1 X. Liu, S. Gao, H. Xu, Z. Lou, W. Wang, B. Huang and Y. Dai, *Nanoscale*, 2013, **5**, 1870–1875.
2 T.-S. Yang, M.-C. Yang, C.-B. Shiu, W.-K. Chang and M.-S. Wong, *Appl. Surf. Sci.*, 2006, **252**, 3729–3736.
3 L. Si, Z. Huang, K. Lv, D. Tang and C. Yang, *J. Alloys Compd.*, 2014, **601**, 88–93.